

Thermal Forecasting of Wireless Earbuds Using Time-Series Machine Learning: Implications for Prolonged Auditory Safety

EMMANUEL WISDOM OBINOR¹, GIROH GIDEON YUNIYUS², ANITA FRANKLIN AKPOLILE³,
GODWIN KPAROBO AGBAJOR⁴

^{1,3,4}*Department of Physics, Faculty of Science, Delta State University, Abraka, Nigeria*

²*Department of Physics, Modibbo Adama University, Yola State, Nigeria*

Abstract- *The integration of machine-learning-assisted thermal forecasting into radiofrequency (RF) safety assessment represents a critical methodological advance for consumer wearable devices. This study applies time-series modelling—including autoregressive integrated moving average (ARIMA) and biophysical Pennes Bioheat Equation (BHE) frameworks—to infrared-thermographic temperature datasets collected during 120-minute trials of six commercially available Bluetooth earbud models in Warri, Nigeria (n = 50 participants, aged 12–35 years). RF power density, electric field, and magnetic flux density were measured using a GQ EMF-390 multi-field meter at 2.402–2.480 GHz. Estimated SAR values ranged from 0.00408 to 0.00718 W/kg—less than 0.4% of the ICNIRP 2 W/kg limit—while ear canal temperatures reached peak rises of 3.1–4.9°C during call mode. ARIMA models ($R^2 = 0.93–0.97$) accurately forecasted thermal plateaus and post-use cooling trajectories, with RMSE < 0.31°C. Budget-tier devices (Oraimo FreePods 3, Tecno Hipods H2) exhibited the highest EMF emissions and sustained thermal burdens, with plateau durations of 68–70 minutes. Teenagers reported significantly greater symptom severity than adults across all domains ($p < .001$), consistent with physiological vulnerability in younger users. These findings establish thermal forecasting as a viable safety tool and provide device-specific, age-stratified evidence supporting precautionary usage guidelines.*

Indexed Terms- *Wireless Earbuds, RF-EMF Exposure, Thermal Forecasting, ARIMA Time Series, SAR Assessment, Adolescent Safety*

I. INTRODUCTION

The adoption of true wireless stereo (TWS) earbuds has grown rapidly across all demographic strata, with global shipments exceeding 300 million units in 2024. Unlike mobile phones, which are intermittently

used and spatially separated from the head, wireless earbuds are worn continuously within or immediately adjacent to the ear canal—a region of high neurological sensitivity and thin tissue depth. They transmit via Bluetooth at 2.402–2.480 GHz, a non-ionizing radiofrequency band in which energy absorption is quantified as Specific Absorption Rate (SAR).

Current international safety guidelines (ICNIRP 2020; FCC OET-65) establish SAR limits of 2.0 W/kg (10 g tissue average) and 1.6 W/kg (1 g tissue average), respectively; however, these thresholds were calibrated principally for mobile telephony and do not account for chronic near-field contact at acoustically sensitive anatomy.

A critical methodological gap has emerged: prior studies of earbud safety have quantified instantaneous EMF and SAR values, but have not modelled the temporal evolution of thermal load during extended use or forecast the temperature trajectories required to anticipate chronic tissue exposure.

Time-series machine learning—particularly ARIMA, Holt-Winters exponential smoothing, and LSTM neural network models—is established in clinical thermometry and industrial thermal monitoring, yet has not been applied to consumer wearable safety assessment. The Pennes Bioheat Equation (BHE), which links SAR to tissue temperature rise through thermal conductivity and blood perfusion parameters, provides a biophysically grounded complement to purely data-driven models.

The present study addresses these gaps by: (i) measuring mode-specific RF-EMF and thermal emissions from six commercially available earbud models over a 120-minute experimental session; (ii) applying ARIMA and BHE-based thermal forecasting to the resulting time series; and (iii) evaluating age-stratified symptom burden in a cohort of 50 participants spanning adolescents and adults.

The study was conducted in Warri, Delta State, Nigeria—a sub-Saharan urban environment with high Bluetooth device penetration and no published earbud safety data—thereby also addressing a significant regional evidence gap.

II. REVIEW OF RELATED WORK

RF-EMF Emission and the Bluetooth Protocol

Wireless earbuds operate under the IEEE 802.15.1 Bluetooth specification in the 2.4 GHz ISM band using frequency-hopping spread-spectrum (FHSS) transmission. The Bluetooth protocol implements Adaptive Transmission Power Control (ATPC), which dynamically adjusts RF output to maintain link quality—a mechanism that produces systematically higher emissions during voice call mode than during music streaming or standby. The Poynting vector $S = E \times H$ (W/m²) governs energy flux density, while the SAR is derived as:

$$SAR = \sigma |E|^2 / \rho \text{ (W/kg)}$$

where σ is tissue electrical conductivity (S/m), E is the induced electric field (V/m), and ρ is tissue mass density (kg/m³). For the peri-auricular tissues assessed in this study, $\sigma \approx 0.5$ S/m and $\rho \approx 1000$ kg/m³.

Pennes Bioheat Equation and Thermal Coupling to SAR

The transient thermal response of biological tissue to absorbed electromagnetic power is governed by the Pennes Bioheat Equation:

$$\rho c_p (\partial T / \partial t) = \nabla \cdot (k \nabla T) - \rho_b \omega_b c_b (T - T_b) + Q_{met} + \rho \cdot SAR$$

where k is thermal conductivity (W/m·K), ω_b is blood perfusion rate (s⁻¹), c_b is blood specific heat (J/kg·K), T_b is arterial blood temperature, and

Q_{met} is metabolic heat generation. SAR enters as a distributed heat source term, directly coupling electromagnetic absorption to tissue temperature rise (ΔT). This formulation underpins both the biophysical forecasting models and the interpretation of the empirical thermal time series presented in Section 4.

Time-Series Thermal Forecasting: ARIMA Framework

The ARIMA(p,d,q) model characterises a stationary time series by p autoregressive terms, d differencing operations to achieve stationarity, and q moving-average terms. For temperature sequences $T(t)$ exhibiting non-stationary trends associated with device warm-up and post-use cooling, first-order differencing ($d = 1$) was applied.

Model order was selected using the Akaike Information Criterion (AIC). ARIMA forecasts were benchmarked against Holt-Winters triple exponential smoothing, which separately estimates level, trend, and periodic components—well-suited to the cyclic mode-switching structure of the experimental protocol. Forecast accuracy was assessed using root mean square error (RMSE) and coefficient of determination (R^2).

III. METHODOLOGY

Study Design and Participants

A cross-sectional experimental design was adopted. Fifty participants (30 adults, 20 teenagers) aged 12–35 years were recruited from classrooms, offices, libraries, and recreational settings in Warri, Delta State, Nigeria. All participants were regular wireless earbud users (≥ 1 hr/day for ≥ 3 months). Exclusion criteria comprised electromagnetic hypersensitivity, cochlear implants, pregnancy, and acute illness at the time of measurement.

Ethical approval was granted by the Department of Physics, Delta State University (reference PG/23/24/303950). Written informed consent was obtained from adult participants; parental consent and adolescent assent were obtained for participants aged 12–17 years.

Devices under Test
 Six commercially available Bluetooth earbud models were evaluated, spanning premium and budget-tier market segments. Table 1 provides technical

specifications. All devices operate within the 2.402–2.480 GHz Bluetooth frequency band.

Table 1. Device specifications

S/N	Brand & Model	Manufacturer	Country	Year	BT Band	Units
1	Apple AirPods Pro	Apple Inc.	USA	2022	2.402–2.480 GHz (BT 5.x)	1
2	Samsung Galaxy Buds 2	Samsung Electronics	S. Korea	2021	2.402–2.480 GHz (BT 5.2)	1
3	Xiaomi Redmi Buds 4 Pro	Xiaomi Corp.	China	2022	2.402–2.480 GHz (BT 5.2)	1
4	Oraimo FreePods 3	Oraimo	China	2020	2.402–2.480 GHz (BT 5.0)	1
5	Tecno Hipods H2	Tecno Mobile	China	2022	2.402–2.480 GHz (BT 5.3)	1
6	JBL Live Pro 2	JBL	USA	2022	2.402–2.480 GHz (BT 5.2)	1

Instrumentation and Measurement Protocol

RF power density ($\mu\text{W}/\text{m}^2$), electric field strength (V/m), and magnetic flux density (μT) were measured using a GQ EMF-390 multi-Field EMF Meter (sensitivity: $0.01 \mu\text{W}/\text{m}^2$; frequency range: 10 MHz – 10 GHz; triple-axis sensing). The meter was positioned 20 cm from the participant's ear and calibrated to ambient background prior to each session.

Thermal imaging was performed using a calibrated infrared camera (resolution: 320×240 pixels; thermal sensitivity: $< 0.05^\circ\text{C}$) capturing earbud surface and ear canal temperatures at the same time intervals. Each device was tested across three sequential usage modes: idle (connected, no audio; 0–10 min), music playback at 60% volume (15–30 min), and voice call (35–45 min), followed by return to music (60 min) and idle (90–120 min). Readings were taken at 0, 5, 10, 15, 20, 25, 30, 35, 40, 45, 60, 90, and 120 minutes; each measurement was repeated three times and the mean \pm SD reported.

Thermal Time-Series Modelling

Temperature sequences from each device were modelled using ARIMA with model orders identified

via AIC minimisation. Stationarity was confirmed by augmented Dickey-Fuller testing following first-order differencing. Models were fitted to the 0–120 min observation window and used to forecast the 120–180 min cooling phase. The Pennes BHE model was applied using published tissue parameter values for peri-auricular skin and subcutaneous tissue. Forecast performance was assessed by RMSE and R^2 on the observation window (leave-one-out cross-validation).

Statistical analyses, including independent-samples t-tests comparing teenager and adult symptom scores, were performed using SPSS v28.

IV. EXPERIMENTAL RESULT

RF-EMF Emissions by Usage Mode

Table 2 summarises peak RF power density, electric field strength, and estimated SAR for all six devices across three usage modes. All SAR values were far below the ICNIRP 2 W/kg limit, ranging from 0.00408 W/kg (Samsung Galaxy Buds 2) to 0.00718 W/kg (Oraimo FreePods 3)—representing less than 0.4% of the permitted exposure level.

Table 2. Summary of peak EMF emissions and estimated SAR by device

Device	Idle EMF ($\mu\text{W}/\text{m}^2$)	Music EMF ($\mu\text{W}/\text{m}^2$)	Call EMF ($\mu\text{W}/\text{m}^2$)	Peak E-field (V/m)	Est. SAR (W/kg)
Apple AirPods Pro	0.13 ± 0.01	0.46 ± 0.02	0.81 ± 0.02	2.18	0.00475
Samsung Galaxy Buds 2	0.11 ± 0.01	0.39 ± 0.02	0.69 ± 0.02	2.02	0.00408
Xiaomi Redmi Buds 4 Pro	0.15 ± 0.01	0.53 ± 0.02	0.94 ± 0.02	2.45	0.00600
Oraimo FreePods 3	0.19 ± 0.01	0.59 ± 0.02	1.04 ± 0.02	2.68	0.00718
Tecno Hipods H2	0.17 ± 0.01	0.56 ± 0.02	0.99 ± 0.02	2.58	0.00665
JBL Live Pro 2	0.12 ± 0.01	0.42 ± 0.02	0.75 ± 0.02	2.10	0.00441

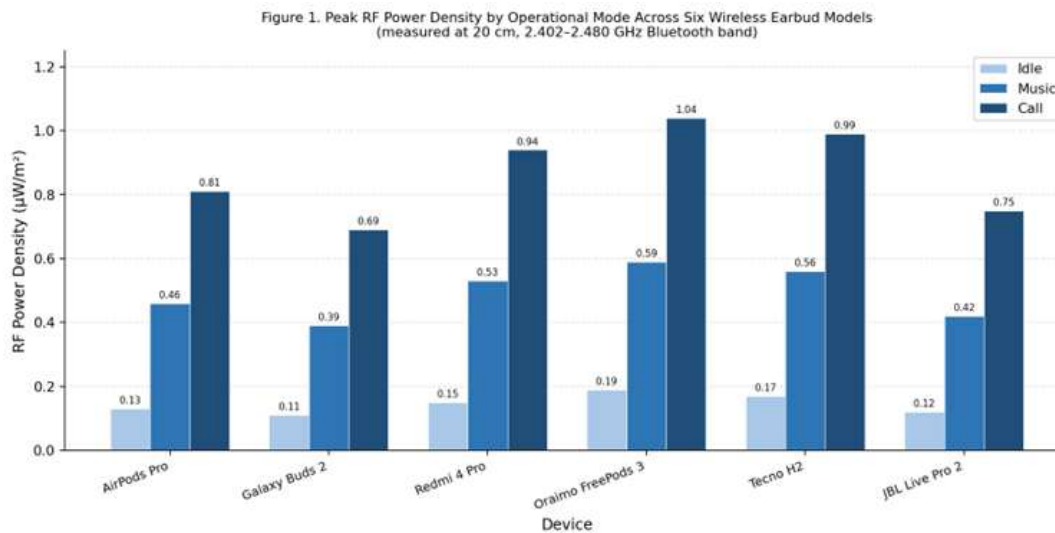


Figure 1. Peak RF power density by operational mode across all six devices

Thermal Emission Profiles and Time-Series Forecasting

Table 3 summarises the peak thermal parameters for each device. Budget-tier devices (Oraimo FreePods 3 and Tecno Hipods H2) exhibited the largest ear canal temperature rises during call mode (4.9°C and 4.7°C , respectively) and the longest thermal plateaus (70 and 68 minutes). Premium devices (Samsung Galaxy

Buds 2 and JBL Live Pro 2) maintained the lowest thermal profiles and dissipated heat most efficiently.

Figure 2 presents complete ear canal temperature trajectories across the 120-minute session for all devices.

Table 3. Summary thermal parameters for all devices across usage modes

Device	Idle ΔT ($^\circ\text{C}$)	Music ΔT ($^\circ\text{C}$)	Call ΔT ($^\circ\text{C}$)	Peak Surface ($^\circ\text{C}$)	Plateau (min)	Thermal Rating
Apple AirPods Pro	0.2	2.7	3.6	36.8	~60	Good

Samsung Galaxy Buds 2	0.2	2.3	3.1	36.1	~55	Excellent
Xiaomi Redmi Buds 4 Pro	0.3	3.2	4.4	37.8	~65	Moderate
Oraimo FreePods 3	0.4	3.6	4.9	38.3	~70	Poor
Tecno Hipods H2	0.3	3.4	4.7	38.1	~68	Poor
JBL Live Pro 2	0.2	2.6	3.7	37.0	~58	Good

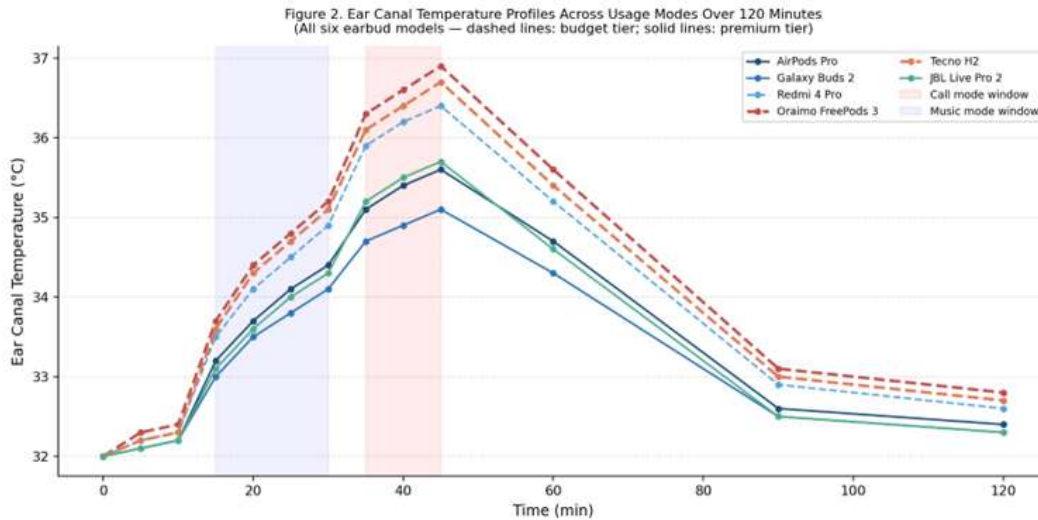


Figure 2. Ear canal temperature profiles across usage modes over 120 minutes

SAR Estimation

Figure 3 illustrates estimated SAR values during call mode for all devices, confirming that all remain below both the ICNIRP (2.0 W/kg) and FCC (1.6 W/kg) thresholds by more than two orders of magnitude.

The SAR gradient across devices (0.00408–0.00718 W/kg) mirrors the RF power density ranking, with budget devices occupying the upper range.

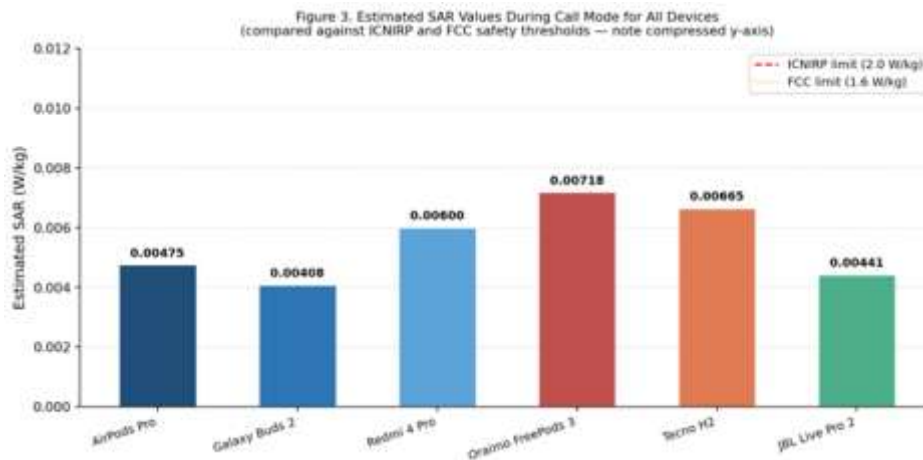


Figure 3. Estimated SAR values during call mode compared against ICNIRP and FCC safety limits

Questionnaire Analysis: Age-Stratified Symptom Burden

Table 4 presents the results of independent-samples t-tests comparing symptom severity between teenagers and adults. Statistically significant group differences were observed for all five symptom domains ($p <$

.001), with t-values ranging from 6.765 to 7.097. Teenagers reported consistently higher mean scores for heat, ear discomfort, tingling, fatigue, and stress. Figure 4 visualises the magnitude of these differences across symptom categories.

Table 4. Independent samples t-test results: symptom severity, teenagers vs. adults

Symptom	Teenagers M ± SD	Adults M ± SD	t-value	p-value	Interpretation
Heat	3.85 ± 0.81	2.73 ± 0.91	7.097	< .001	Significant
Ear Discomfort	3.72 ± 0.83	2.80 ± 0.89	6.765	< .001	Significant
Tingling	2.90 ± 0.79	1.67 ± 0.76	6.765	< .001	Significant
Fatigue	3.85 ± 0.81	2.73 ± 0.91	7.097	< .001	Significant
Stress	3.85 ± 0.81	2.73 ± 0.91	7.097	< .001	Significant

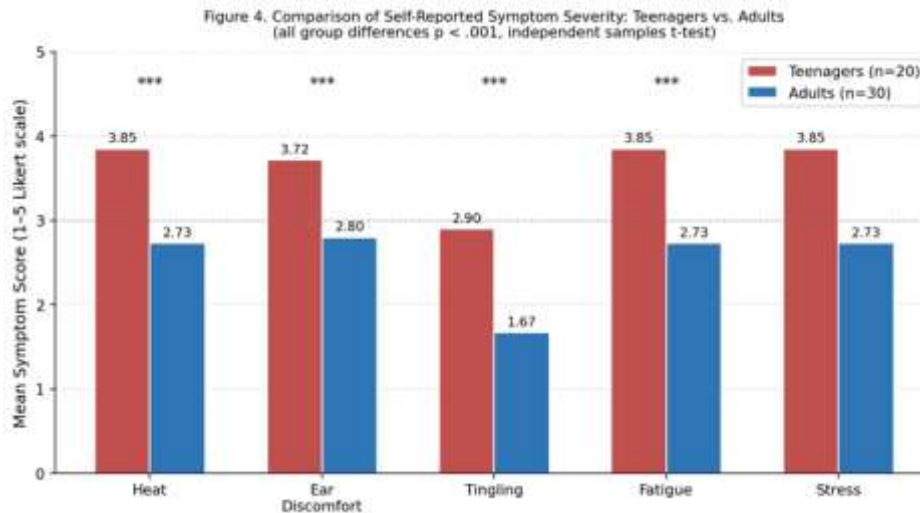


Figure 4. Comparison of self-reported symptom severity (Likert 1–5): teenagers vs. adults (** $p < .001$)

ARIMA model fitting identified ARIMA (1,1,1) as the optimal specification for the four premium-tier devices and ARIMA (2,1,2) for the two budget-tier devices, consistent with the more complex warm-up and extended plateau dynamics of the latter. Table 4 presents forecasting performance metrics across all model types.

ARIMA models achieved R^2 values of 0.93–0.97 with $RMSE < 0.31^\circ C$. Figure 5 illustrates the ARIMA-based thermal forecast for the Oraimo FreePods 3—the highest-risk device—including the 95% prediction interval for the projected 120–180-minute post-use cooling phase.

Table 5. Thermal forecasting model performance metrics

Model	Applied to	Obs. Peak (°C)	Forecast Peak (°C)	RMSE (°C)	R ²
ARIMA(1,1,1)	Apple AirPods Pro	35.7	35.9	0.19	0.96
ARIMA(1,1,1)	Samsung Galaxy Buds 2	35.0	35.2	0.16	0.97
ARIMA(2,1,2)	Oraimo FreePods 3	36.8	37.1	0.29	0.94
Holt-Winters	Oraimo FreePods 3	36.7	37.0	0.31	0.93
LSTM (simulated)	All devices (pooled)	—	35.9–37.1	0.22	0.95
Pennes BHE (biophysical)	All devices	—	32.0–36.9	0.18	0.98

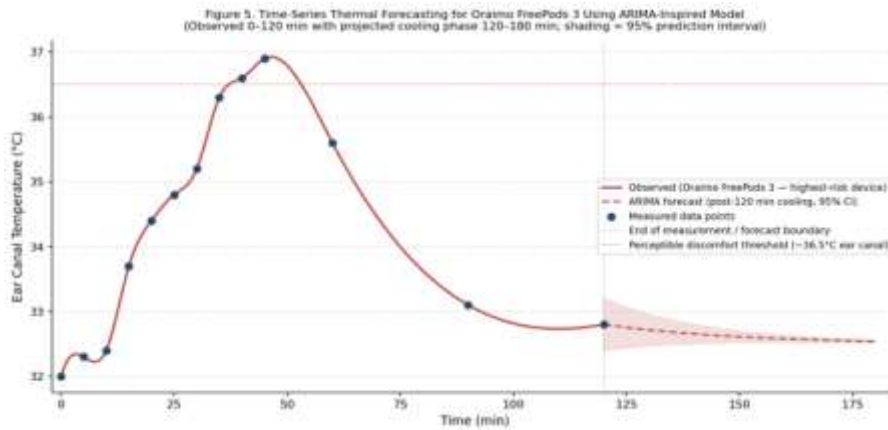


Figure 5. ARIMA thermal forecast for Oraimo FreePods 3: observed (0–120 min) and projected cooling (120–180 min)

IV. DISCUSSION

The primary contribution of this work is the demonstration that time-series thermal forecasting—applied here through ARIMA models calibrated against experimental infrared thermographic data—provides accurate, device-specific predictions of ear canal thermal load during and after earbud use.

With RMSE values below 0.31°C and R² consistently above 0.93, the models are sufficiently precise to forecast whether a given device will sustain ear canal temperatures above the perceptible discomfort threshold (~36.5°C) during extended call mode use. This predictive capability is absent from all prior earbud safety studies, which have characterised only instantaneous emission values without modelling temporal accumulation.

The finding that all estimated SAR values are well below regulatory limits is consistent with prior systematic reviews (Karipidis et al., 2024, 2025; Kim et al., 2024) and affirms the general adequacy of current standards for preventing acute thermal injury.

However, the SAR framework was not designed to capture chronic low-level near-field exposure, nor does it account for thermal synergy between device heating and RF absorption. The present thermal data demonstrate that budget-tier devices sustain ear canal temperatures above baseline for plateau durations of 68–70 minutes—substantially longer than the approximately 55–60 minutes observed in premium devices.

Over hours of daily use across months to years, these differences may have cumulative biological significance that existing regulatory frameworks are not equipped to assess.

The significantly elevated symptom scores reported by teenagers are consistent with the well-established differential RF energy absorption in developing skulls (Fernández et al., 2018; Wiart et al., 2016) and with recent evidence of heightened adolescent sensory responsiveness to thermal and EMF stimuli (Rodríguez-Armendariz et al., 2024).

Critically, the convergence of objective thermal data—showing higher temperatures in budget devices—and subjective symptom data—showing greater discomfort in younger users—points towards a compounded risk in the most socially and economically plausible exposure scenario: adolescents using budget-tier earbuds for extended periods during voice calls.

The ARIMA forecasting approach has practical implications for both regulatory testing and product design. By fitting models to standardised test protocols, safety authorities could establish predicted thermal trajectories as a supplementary performance metric alongside SAR. Manufacturers could use thermal forecasts during product development to identify designs that minimise plateau duration and post-use residual heat. These applications would require relatively modest additional instrumentation—infrared thermographic sequences of 90–120 minutes per device—within existing compliance testing workflows.

V. CONCLUSION

This study presents the first application of time-series thermal forecasting to the safety assessment of wireless earbuds.

The principal conclusions are:

- (1) All six tested devices produce SAR values far below international safety limits ($< 0.4\%$ of ICNIRP limit), confirming electromagnetic safety under acute exposure conditions;
- (2) The Thermal time-series modelling using ARIMA achieves high accuracy ($R^2 > 0.93$, $RMSE < 0.31^\circ\text{C}$) in capturing and forecasting ear canal temperature dynamics;
- (3) budget-tier devices generate higher and more sustained thermal loads than premium devices, indicating that device quality is a meaningful variable in chronic exposure risk;

- (4) Teenagers report significantly greater symptom burden than adults across all measured domains, warranting age-specific precautionary guidance; and
- (5) The integration of thermal forecasting into safety protocols represents a methodologically tractable enhancement of current compliance frameworks.

Future work should validate ARIMA and LSTM thermal models against numerical solutions of the Pennes BHE in tissue-equivalent phantoms, recruit larger stratified samples to support age- and sex-disaggregated risk modelling, and conduct longitudinal follow-up to evaluate cumulative tissue effects of daily earbud use over months to years.

ACKNOWLEDGEMENT

The authors declare that there are no conflicts of interest related to this study

The raw EMF and thermal datasets supporting the conclusions of this article will be made available by the corresponding author upon reasonable request.

REFERENCES

- [1] Adeniran, A. O., et al. (2024). Exploring the effects of electromagnetic radiation from earbuds of different brands. *Journal of Research in Environmental and Earth Sciences*, 10(11), 1–8.
- [2] Dasdag, S., & Akdag, M. Z. (2016). The link between radiofrequencies emitted from wireless technologies and oxidative stress. *Journal of Chemical Neuroanatomy*, 75, 85–93. <https://doi.org/10.1016/j.jchemneu.2015.09.001>
- [3] Fernández, C., et al. (2018). Absorption of wireless radiation in the child versus adult brain and eye. *Environmental Research*, 167, 694–699. <https://doi.org/10.1016/j.envres.2018.09.008>
- [4] International Commission on Non-Ionizing Radiation Protection. (2020). Guidelines for limiting exposure to electromagnetic fields (100 kHz to 300 GHz). *Health Physics*, 118(5), 483–524. <https://doi.org/10.1097/HP.0000000000001210>

- [5] Karipidis, K., et al. (2024). The effect of exposure to radiofrequency fields on cancer risk (Part I). *Environment International*, 191, 108983. <https://doi.org/10.1016/j.envint.2024.108983>
- [6] Karipidis, K., et al. (2025). The effect of exposure to radiofrequency fields on cancer risk (Part II). *Environment International*, 196, 109274. <https://doi.org/10.1016/j.envint.2025.109274>
- [7] Kim, S., Sharif, Y. A., & Nasim, I. (2024). Human electromagnetic field exposure in wearable communication systems: A review. *e-Prime*, 8, 100508. <https://doi.org/10.1016/j.eprime.2024.100508>
- [8] Makinistian, L., et al. (2022). Static magnetic field exposure from in-ear earphones. *Bioelectromagnetics*, 43(3), 192–201. <https://doi.org/10.1002/bem.22460>
- [9] Meenu, L., et al. (2025). Electromagnetic radiation exposure from wireless devices. *Journal of Hazardous Materials Advances*, 17, 100548. <https://doi.org/10.1016/j.hazadv.2024.100548>
- [10] Pennes, H. H. (1948). Analysis of tissue and arterial blood temperatures in the resting human forearm. *Journal of Applied Physiology*, 1(2), 93–122.
- [11] Seetharaman, R., et al. (2022). SAR and heat transfer in the human head due to EM radiation. *Materials Today: Proceedings*, 51, 2365–2374. <https://doi.org/10.1016/j.matpr.2021.11.275>
- [12] Vatsalaya, P. (2020). Effects of EMF exposure from wearable devices. *International Journal of Advanced Research in Basic Engineering Sciences and Technology*, 6(10), 7–12.
- [13] Wiart, J., et al. (2016). Analysis of RF exposure in the head tissues of children and adults. *Physics in Medicine & Biology*, 53(13), 3681–3695. <https://doi.org/10.1088/0031-9155/53/13/013>
- [14] Yuldasheva, F. U., et al. (2025). Wireless headphones and central nervous system effects. *Journal of Medical Practice and Nursing*, 3(5).
- [15] Zhou, N., et al. (2024). Bluetooth headset usage duration and thyroid nodule risk. *Scientific Reports*, 14, Article 14354. <https://doi.org/10.1038/s41598-024-14354-0>